PHOTONICS Research

Highly efficient transparent quantum-dot light-emitting diodes based on inorganic double electron-transport layers

Nan Zhang,[1] Xiangwei Qu,[2,3] Quan Lyu,[4] Kai Wang,[2,3,5] and Xiao Wei Sun[2,3,6]

[1]Peng Cheng Laboratory, Shenzhen 518055, China
[2]Guangdong University Key Laboratory for Advanced Quantum Dot Displays and Lighting, Guangdong-Hong Kong-Macao Joint Laboratory for Photonic-Thermal-Electrical Energy Materials and Devices, and Department of Electrical and Electronic Engineering, Southern University of Science and Technology, Shenzhen 518055, China
[3]Key Laboratory of Energy Conversion and Storage Technologies (Southern University of Science and Technology), Ministry of Education, Shenzhen 518055, China
[4]Huawei Technologies Research & Development (UK) Ltd., Ipswich IP5 3RE, UK
[5]e-mail: wangk@sustech.edu.cn
[6]e-mail: sunxw@sustech.edu.cn

Received 8 April 2021; revised 24 July 2021; accepted 13 August 2021; posted 13 August 2021 (Doc. ID 424750); published 15 September 2021

Herein, we report the fabrication of high-performance transparent quantum-dot light-emitting diodes (Tr-QLEDs) with ZnO/ZnMgO inorganic double electron-transport layers (ETLs). The ETLs effectively suppress the excess electron injection and facilitate charge balance in the Tr-QLEDs. The thick ETLs as buffer layers can also withstand the plasma-induced damage during the indium tin oxide sputtering. These factors collectively contribute to the development of Tr-QLEDs with improved performance. As a result, our Tr-QLEDs with double ETLs exhibited a high transmittance of 82% at 550 nm and a record external quantum efficiency of 11.8%, which is 1.27 times higher than that of the devices with pure ZnO ETL. These results indicate that the developed ZnO/ZnMgO inorganic double ETLs could offer promising solutions for realizing high-efficiency Tr-QLEDs for next-generation display devices. © 2021 Chinese Laser Press

https://doi.org/10.1364/PRJ.424750

1. INTRODUCTION

Optoelectronics is one of the cornerstone technologies that promoted the rapid development of modern society's new and smart infrastructure. In the past few decades, optoelectronic devices have entered into the field of consumer electronic products and information industry on a large scale, thereby changing the lifestyle of the masses. One such next-generation device—transparent quantum-dot light-emitting diodes (Tr-QLEDs)—have attracted extensive attention as a potential candidate for transparent display technology owing to their unique characteristics such as size-dependent tunable wavelength emission, narrow linewidth, high color saturation, high electroluminescence (EL) efficiency, high stability, and solution-processed fabrication [1–5]. Traditional LEDs, including QLEDs, organic LEDs (OLEDs), and perovskite LEDs, are opaque because their top electrodes [6] are fabricated with highly reflective metal thin films (Al, Cu, Ag, or Au). Since the first report on QLEDs in 1994 [7], considerable advances have been made in the device performance; especially the stability, lifetime, color saturation, and EL efficiency of the QLEDs have become comparable to those of the OLEDs [2]. However, despite the remarkable progress made in improving the QLED performance, the performance of the transparent LEDs is still lower than that of the nontransparent LEDs, owing to imbalanced carrier injection, energy-level mismatch, damage due to plasma sputtering, and poor conductivity of the top transparent electrodes [8–11].

In the past decade, several studies were conducted to identify plausible methods to improve the performance of Tr-QLEDs. For instance, Kim and co-workers first reported a semitransparent inverted QLED fabricated using a red quantum-dot emissive layer (QD EML). This device exhibited a maximum luminance of 10540 cd/m^2 and peak transparency of approximately 45% in the red region of the visible spectrum [8]. Though these inverted Tr-QLEDs can be easily connected with thin-film transistors made of amorphous Si or an n-type metal oxide, the current efficiency of these devices is much lower than that of the devices with conventional architecture [10]. Recently, a hybrid anode [Ag nanowires (NWs) and Al-doped ZnO] has been reportedly used in an inverted Tr-QLED [12], which showed a current efficiency of 15.33 cd/A and transmittance of 75.66% at 530 nm. However, in this

device, poly(9-vinlycarbazole) dissolved in toluene was used as the hole transport layer (HTL), which can damage the underlying quantum dot (QD) layer, thus lowering the device performance.

Compared to the inverted Tr-QLEDs, the conventional Tr-QLEDs tend to exhibit better EL characteristics. For example, Wang and co-workers developed a highly transparent QLED using thick ZnO nanocrystals to prepare the buffer layer and electron transport layer (ETL) [13]. The resulting Tr-QLED with a high average transparency of 70% exhibited an external quantum efficiency (EQE) of 5% (current efficiency of 7 cd/A), which was comparable to that of the devices with conventional Al electrodes. In 2015, a Tr-QLED, developed using a vacuum-free fabrication process and containing an Ag NW cathode, was demonstrated. This device exhibited a reported luminance and current efficiency of over $20,000\ \mathrm{cd/m^2}$ and 5.2 cd/A, respectively [14]. A recent study has shown that by controlling the interface morphology of the ETL while assembling a Tr-QLED [15,16], the surface quenching, electron/hole injection balance, and energy-level matching can be further improved to realize a high-performance Tr-QLED with a peak EQE of 10.63% [16]. Despite these advances, the characteristics of the Tr-QLEDs reported to date are not comparable to those of the traditional nontransparent QLEDs, and hence, the Tr-QLEDs, in their present form, cannot meet the demands of next-generation transparent display technology.

Herein, we introduce efficient ZnO/ZnMgO inorganic double ETLs to achieve Tr-QLEDs with highly improved EL characteristics. In the previously reported studies, organic/inorganic double ETLs [17], double metal oxide (ZnO/SnO_2) ETLs [18], and ZnMgO:ZnO composite ETL were applied to improve the charge balance and obtain high-performance nontransparent QLEDs [19]. However, a Tr-QLED based on inorganic double ETLs remains hitherto unexplored. Thus, in this work, we developed high-performance Tr-QLEDs by utilizing ZnO/ZnMgO inorganic double ETLs and demonstrated that such double ETLs can prevent excess electron injection from the transparent cathode, promote charge balance, and reduce damage caused by plasma sputtering. These factors effectively improved the EL characteristics of the Tr-QLEDs.

2. EXPERIMENT

For this experiment, the red CdSe/ZnS QDs were purchased from Suzhou Xingshuo Nanotech Co., Ltd., and the ZnO and ZnMgO nanoparticles were procured from Guangdong Poly Opto-Electronics Co., Ltd. The organic semiconductors, including poly(3,4-ethylenedioxythiophene):poly(styrenesulfonate) (PEDOT:PSS) and poly(9,9-dioctylfluorene-co-N-(4-(3-methyl-propyl))diphenylamine) (TFB), were obtained from Luminescence Technology Corp. The patterned indium tin oxide (ITO) substrates were cleaned using an ultrasonic cleaner in which first acetone, followed by ethanol, and, finally, deionized water were used to achieve a clean surface. Next, the ITO glass was UV-ozone treated for 20 min. PEDOT:PSS (Baytron PVP Al 4083; filtered through a 0.45 mm filter) was spin coated onto the cleaned ITO glass at 3000 r/min for 45 s, and the coated glass was baked at 130°C for 15 min. Next, a layer of TFB (dissolved in chlorobenzene; 8 mg/mL) was spin coated on the previously deposited PEDOT:PSS layer at 4000 r/min for 45 s and subsequently baked at 120°C for 10 min. Third, a layer of the red QDs (dissolved in octane; 13 mg/mL) was spin coated at 4000 r/min for 45 s and baked at 100°C for 5 min. This was followed by spin coating the ZnO nanoparticles (dissolved in ethanol; 20 mg/mL) at 2000 r/min for 45 s and subsequent baking at 80°C for 20 min. After that, ZnMgO nanoparticles (dissolved in ethanol; 10 mg/mL) were spin coated, as the fifth layer, at 4000 r/min for 45 s, followed by baking at 100°C for 10 min. The thicknesses of the ZnO and ZnMgO layers were 30 and 10 nm, respectively. Finally, a top ITO electrode was deposited by magnetron sputtering at a working pressure of 0.67 Pa, power of 50 W, argon flow of 20 sccm (standard cubic centimeters per minute), and deposition time of 20 min. All the measurements were performed in air at room temperature. Details of the device characterizations are described elsewhere [20,21].

3. RESULTS AND DISCUSSION

We fabricated Tr-QLEDs, each with a structure of ITO/PEDOT:PSS/TFB/QDs/ZnO/ZnMgO/ITO, to evaluate the effect of double ETLs on the device performance. In this structure, the bottom ITO electrode, PEDOT:PSS layer, TFB layer, QD layer, ZnO/ZnMgO layers, and top ITO layer acted as the anode, hole injection layer, HTL, emission layer, double ETLs, and cathode, respectively [Fig. 1(a)].

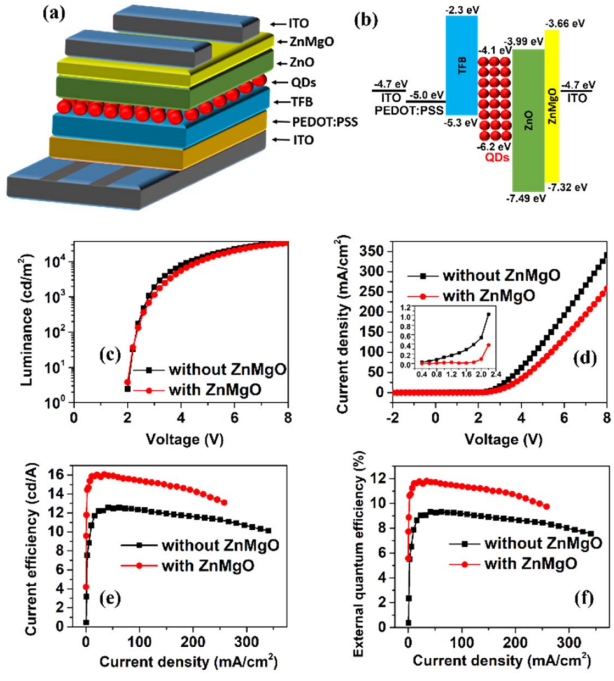

Fig. 1. (a) Structural design and (b) the corresponding energy level diagram of the Tr-QLEDs fabricated in this study [22]. Performance of the fabricated Tr-QLED device: (c) luminance–voltage (L–V) characteristics, (d) current density–voltage (J–V) characteristics, and (e) current efficiency and (f) EQE as functions of current density.

Figure 1(b) shows the energy levels of the Tr-QLEDs fabricated in this work [22]. In these Tr-QLEDs, we used TFB as the HTL because of its hole mobility (10^{-2} $cm^2 \cdot V^{-1} \cdot s^{-1}$), which is higher than that of poly-N-vinylcarbazole (PVK) (2.5×10^{-6} $cm^2 \cdot V^{-1} \cdot s^{-1}$) and poly(4-butylphenyl-diphenylamine) (1×10^{-4} $cm^2 \cdot V^{-1} \cdot s^{-1}$) [23–25]. Further, we used ZnO and ZnMgO nanoparticle layers as the double ETLs because of their higher electron mobility and shallower lowest unoccupied molecular orbitals [19]. Figures 1(c)–1(f) display the luminance–voltage (L–V) and current density–voltage (J–V) characteristics as well as the current efficiency and EQE of the fabricated Tr-QLEDs without and with ZnMgO. Figure 1(c) indicates that the Tr-QLEDs with double ETLs and those with a single ETL exhibited similar applied voltage-dependent turn-on voltages and steep increases in luminance. The turn-on voltages of the Tr-QLEDs with and without ZnMgO were both approximately 2 V, as evident from Fig. 1(c). Figure 1(d) shows the current density–voltage (J–V) characteristics of the fabricated Tr-QLEDs. Evidently, the current density of the device decreased due to the double ETLs. The inset graph in Fig. 1(d) shows that the current density at the turn-on voltage of the Tr-QLEDs with double ETLs is remarkably lower than that of the Tr-QLEDs with pure ZnO ETL. The decrease in the current densities indicates that the electron injection is suppressed due to the lower electron mobility of ZnMgO than of ZnO and the higher energy conduction band (CB) of the QDs than of ZnMgO. Zhang and co-workers reported that the CBs of ZnO and ZnMgO lie at 3.5 eV and 3.7 eV, respectively, and the electron mobility of ZnO is 2×10^{-3} $cm^2 \cdot V^{-1} \cdot s^{-1}$, which is higher than that of ZnMgO; the lower electron mobility of ZnMgO is caused by the reduced number of O vacancies [19]. Notably, imbalanced charge injection—mostly excess electron injection—is a critical problem in the QLEDs [26–28]. Therefore, the decreased electron injection observed in our case can result in an improved charge balance. Furthermore, the Tr-QLEDs without ZnMgO had leakage currents [Fig. 1(d)] as indicated by the small differences in the luminance and significant differences in the current densities observed in Figs. 1(c) and 1(d). The leakage current mainly originates from the thinner ZnO layer, which is too fragile to withstand the plasma-sputtering-induced damage during the ITO deposition process. Moreover, the leakage current across the device can lead to exciton quenching, which degrades the device performance [29]. The EL characteristics of the fabricated Tr-QLEDs with different ETL materials are listed in Table 1. Figures 1(e) and 1(f) along with Table 1 show that the maximum current efficiency and EQE of the Tr-QLEDs with double ETLs reached 16 cd/A and 11.8%, respectively. These values are approximately 1.27 times higher than those of the Tr-QLEDs with pure ZnO ETL. These results suggest that leakage current suppression, decrease in electron injection, and charge balance are the main reasons that improve the device performance.

Table 1. EL Characteristics of Tr-QLEDs with Different ETLs

Device	ETL	Peak EQE (%)	Peak CE[a] (cd/A)	Luminance (cd/m^2)
1	ZnO	9.3	12.6	34,461
2	ZnO/ZnMgO	11.8	16.0	33,764

[a]CE: Current efficiency.

To examine the influence of ZnMgO on the electron injection, we fabricated an electron-only device with a structure of ITO/ZnO/QDs/ZnO with and without ZnMgO/ITO. The ZnO layer was deposited on the ITO glass to block the hole injection in this electron-only device. Figure 2(a) indicates that the current density decreased when the ZnMgO layer was added to the device. This implies that the ZnMgO layer suppressed the electron injection in the Tr-QLEDs. In the previously reported QLEDs [15,16], materials like polyvinylpyrrolidone and alumina were used to decrease the electron injection and balance the charge injection into the QDs. Figures 2(b) and 2(c) illustrate the operational mechanism of the electron-only device with and without the ZnMgO layer. When the ZnMgO layer was added to the electron-only device, the electron injection from the ITO electrode to the EML decreased because of the higher electron injection barrier between ZnMgO and ITO. This decrease in the excess injection of electrons facilitated charge balance in the device. The Tr-QLEDs with and without ZnMgO show red emission at 628 nm in Figs. 2(d)–2(g). The Tr-QLEDs with different ETLs under different voltages do not cause the wavelength to shift. The ZnMgO as modified layer restrains the electron injection and improves the charge balance in our Tr-QLEDs, but it did not lead to the Stark effect occurring under the presence of an external electric field, which could also be responsible for the redshift of the EL spectrum [30].

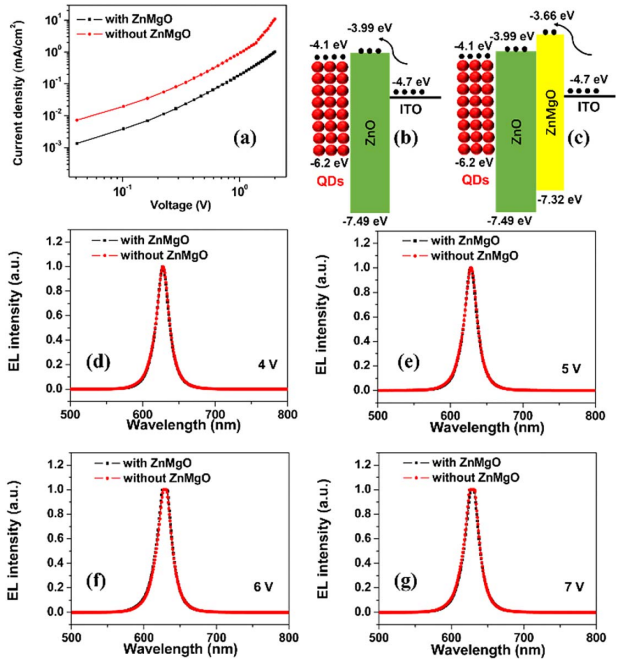

Fig. 2. (a) Current density–voltage (J–V) curves of the electron-only device with and without ZnMgO. Energy-level diagram of the materials and the corresponding working mechanisms of the electron-only devices (b) without and (c) with ZnMgO. (d)–(g) EL spectra of the fabricated Tr-QLEDs device with and without ZnMgO driven by different voltages.

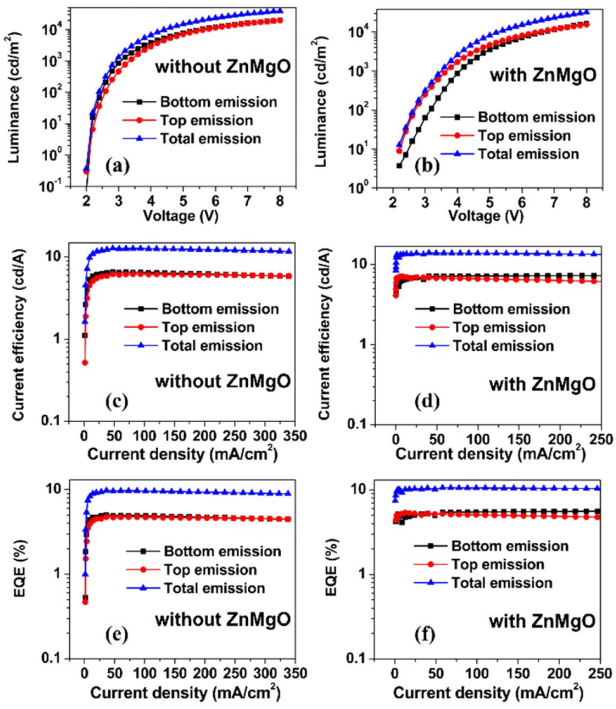

Fig. 3. Bottom, top, and total emission characteristics of Tr-QLEDs without and with a ZnMgO layer: (a) and (b) luminance-voltage (L-V), (c) and (d) current efficiency, (e) and (f) EQE as a function of current density.

We further examined the top and bottom EL characteristics of the devices (Fig. 3). These results showed that the Tr-QLEDs with double ETLs exhibited a maximum EQE of 11.8% for the total light emission, including the bottom and top emissions. This EQE is approximately 27% higher than the EQE of the devices with a single ZnO ETL. According to Table 2, the EQE of our device is the highest reported for Tr-QLEDs to date. Figures 3(a) and 3(b) imply that the bottom and top emissions are equivalent to the order of brightness because of the uniform light extraction capability of the bottom and top ITO electrodes [13,16]. In addition, a thicker ETL as a buffer layer can effectively eliminate the plasma-induced damage to the underlying layers and thus allow a damage-free sputtering process [13]. This leads to the development of highly efficient Tr-QLEDs.

Table 2. Comparison of the Characteristics and Performances of Reported Tr-QLEDs

Device	Maximum EQE (%)	Peak CE[a] (cd/A)	T^b (%)	Luminance (cd/m²)
Ref. [8]	–	1.79	55	10,540
Ref. [9]	–	0.45	75	358
Ref. [10]	–	0.47	74	200
Ref. [12]	–	15.33	75.66[c]	18,407
Ref. [14]	–	10.8	73	48,480
Ref. [16]	10.63	44.23	80	42,610
Our work	11.8	16	82	33,764

[a]CE: Current efficiency.
[b]*T*: Transmittance at 550 nm.
[c]Transmittance at 530 nm.

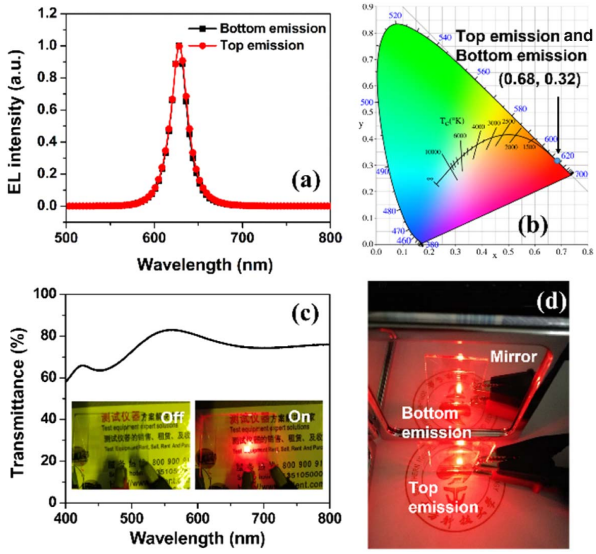

Fig. 4. (a) EL spectra, (b) CIE chromaticity diagram, and (c) transmittance spectra of the fabricated Tr-QLEDs with double ETLs. The inset of (c) shows images of the device at turn-off and turn-on states. (d) Photograph of the Tr-QLED in the front of a mirror.

Figures 4(a) and 4(b) show the EL spectra and CIE *xy* chromaticity diagram (where CIE is the International Committee on Illumination) of the bottom- and top-emitting Tr-QLEDs with double ETLs. Notably, the EL spectrum obtained from the bottom of the device overlaps with that recorded from the top-side of the device, demonstrating a strong uniformity between the light emitted from both sides of the fabricated device. As shown in Fig. 4(c), our Tr-QLEDs exhibited a high transmittance of 82% at 550 nm and an average transmittance of 74% from 400 to 800 nm. The inset of Fig. 4(c) displays the photographs of the turned-off and turned-on transparent devices. The background text can be clearly seen owing to the high brightness and transmittance of the fabricated Tr-QLEDs. Furthermore, we also observed the top and bottom light emissions through a mirror in a dark environment. A very bright and uniform light was emitted from both sides of the device as shown in Fig. 4(d).

4. CONCLUSION

In summary, we demonstrated the fabrication of efficient Tr-QLEDs using ZnO/ZnMgO inorganic double ETLs. These double ETLs can suppress the excess injection of electrons into the EML and improve the charge balance because of the lower electron mobility of ZnMgO and higher electron injection barrier between ZnMgO and the cathode. In addition, the thick double ETLs reduce the plasma-induced damage to the device during the ITO sputtering process. As a result, the Tr-QLEDs with double ETLs exhibited a maximum EQE of 11.8% and a peak current efficiency of 16 cd/A. These values are approximately 1.27 times higher than those of the devices with pure ZnO ETL. These results show that Tr-QLEDs with double ETLs can be a potential solution for the realization and commercial production of high-performance transparent displays.

Funding. National Key Research and Development Program of China (2016YFB0401702, 2017YFE0120400); National Natural Science Foundation of China (61674074, 61704170, 61875082); Natural Science Foundation of Guangdong Province (2017B030306010); Guangdong University Key Laboratory for Advanced Quantum Dot Displays and Lighting (2017KSYS007); Shenzhen Peacock Team Project (KQTD20160301112030005); Development and Reform Commission of Shenzhen Project ([2017]1395).

Disclosures. The authors declare no conflict of interest.

Data Availability. Data underlying the results presented in this paper are not publicly available at this time but may be obtained from the authors upon reasonable request.

REFERENCES

1. A. Castan, H.-M. Kim, and J. Jang, "All-solution-processed inverted quantum-dot light-emitting diodes," ACS Appl. Mater. Interfaces **6**, 2508–2515 (2014).
2. H. Shen, Q. Gao, Y. Zhang, Y. Lin, Q. Lin, Z. Li, L. Chen, Z. Zeng, X. Li, Y. Jia, S. Wang, Z. Du, L. S. Li, and Z. Zhang, "Visible quantum dot light-emitting diodes with simultaneous high brightness and efficiency," Nat. Photonics **13**, 192–197 (2019).
3. L. Wang, J. Lin, Y. Hu, X. Guo, Y. Lv, Z. Tang, J. Zhao, Y. Fan, N. Zhang, Y. Wang, and X. Liu, "Blue quantum dot light-emitting diodes with high electroluminescent efficiency," ACS Appl. Mater. Interfaces **9**, 38755–38760 (2017).
4. P. Shen, F. Cao, H. Wang, B. Wei, F. Wang, X. W. Sun, and X. Yang, "Solution-processed double-junction quantum-dot light-emitting diodes with an EQE of over 40%," ACS Appl. Mater. Interfaces **11**, 1065–1070 (2019).
5. K. Ding, Y. Fang, S. Dong, H. Chen, B. Luo, K. Jiang, H. Gu, L. Fan, S. Liu, B. Hu, and L. Wang, "24.1% external quantum efficiency of flexible quantum dot light-emitting diodes by light extraction of silver nanowire transparent electrodes," Adv. Opt. Mater. **6**, 1800347 (2018).
6. L. Liu, K. Cao, S. Chen, and W. Huang, "Toward see-through optoelectronics: transparent light-emitting diodes and solar cells," Adv. Opt. Mater. **8**, 2001122 (2020).
7. V. L. Colvin, M. C. Schlamp, and A. P. Alivisatos, "Light-emitting-diodes made from cadmium selenide nanocrystals and a semiconducting polymer," Nature **370**, 354–357 (1994).
8. H.-M. Kim, A. R. b. M. Yusoff, T.-W. Kim, Y.-G. Seol, H.-P. Kim, and J. Jang, "Semi-transparent quantum-dot light emitting diodes with an inverted structure," J. Mater. Chem. C **2**, 2259–2265 (2014).
9. J.-T. Seo, J. Han, T. Lim, K.-H. Lee, J. Hwang, H. Yang, and S. Ju, "Fully transparent quantum dot light-emitting diode integrated with graphene anode and cathode," ACS Nano **8**, 12476–12482 (2014).
10. H. Y. Kim, Y. J. Park, J. Kim, C. J. Han, J. Lee, Y. Kim, T. Greco, C. Ippen, A. Wedel, B.-K. Ju, and M. S. Oh, "Transparent InP quantum dot light-emitting diodes with ZrO_2 electron transport layer and indium zinc oxide top electrode," Adv. Funct. Mater. **26**, 3454–3461 (2016).
11. L. Yao, X. Fang, W. Gu, W. Zhai, Y. Wan, X. Xie, W. Xu, X. Pi, G. Ran, and G. Qin, "Fully transparent quantum dot light-emitting diode with a laminated top graphene anode," ACS Appl. Mater. Interfaces **9**, 24005–24010 (2017).
12. X. Jiang, Z. Song, G. Liu, Y. Ma, A. Wang, Y. Guo, and Z. Du, "AgNWs/AZO composite electrode for transparent inverted ZnCdSeS/ZnS quantum dot light-emitting diodes," Nanotechnology **31**, 055201 (2020).
13. W. Wang, H. Peng, and S. Chen, "Highly transparent quantum-dot light-emitting diodes with sputtered indium-tin-oxide electrodes," J. Mater. Chem. C **4**, 1838–1841 (2016).
14. P. Jing, W. Ji, Q. Zeng, D. Li, S. Qu, J. Wang, and D. Zhang, "Vacuum-free transparent quantum dot light-emitting diodes with silver nanowire cathode," Sci. Rep. **5**, 12499 (2015).
15. M. K. Choi, J. Yang, D. C. Kim, Z. Dai, J. Kim, H. Seung, V. S. Kale, S. J. Sung, C. R. Park, N. Lu, T. Hyeon, and D.-H. Kim, "Extremely vivid, highly transparent, and ultrathin quantum dot light-emitting diodes," Adv. Mater. **30**, 1703279 (2018).
16. H. Zhang and S. Chen, "An ZnMgO: PVP inorganic-organic hybrid electron transport layer: towards efficient bottom-emission and transparent quantum dot light-emitting diodes," J. Mater. Chem. C **7**, 2291–2298 (2019).
17. M. Park, J. Song, H. Jung, M. An, J. Lim, C. Lee, J. Roh, and D. Lee, "Improving performance of inverted blue quantum-dot light-emitting diodes by adopting organic/inorganic double electron transport layers," Phys. Status Solidi RRL **14**, 1900737 (2020).
18. M. Park, J. Roh, J. Lim, H. Lee, and D. Lee, "Double metal oxide electron transport layers for colloidal quantum dot light-emitting diodes," Nanomaterials **10**, 726 (2020).
19. Q. Zhang, X. B. Gu, Q. S. Zhang, J. Jiang, X. Jin, F. Li, Z. P. Chen, F. Zhao, and Q. H. Li, "ZnMgO:ZnO composite films for fast electron transport and high charge balance in quantum dot light emitting diodes," Opt. Mater. Express **8**, 909–918 (2018).
20. N. Zhang, S. Ding, K. Wang, Q. Lyu, and W. X. Sun, "Efficient transparent quantum-dot light-emitting diodes with an inverted architecture," Opt. Mater. Express **11**, 2145–2152 (2021).
21. Z. Ren, J. Yu, Z. Qin, J. Wang, J. Sun, C. C. S. Chan, S. Ding, K. Wang, R. Chen, K. S. Wong, X. Lu, W.-J. Yin, and W. C. H. Choy, "High-performance blue perovskite light-emitting diodes enabled by efficient energy transfer between coupled quasi-2D perovskite layers," Adv. Mater. **33**, 2005570 (2021).
22. Y. Sun, Y. Jiang, H. Peng, J. Wei, S. Zhang, and S. Chen, "Efficient quantum dot light-emitting diodes with a $Zn_{0.85}Mg_{0.15}O$ interfacial modification layer," Nanoscale **9**, 8962–8969 (2017).
23. Y. S. Zhao, L. X. Chen, J. L. Wu, X. W. Tan, Z. H. Xiong, and Y. L. Lei, "Composite hole transport layer consisting of high-mobility polymer and small molecule with deep-lying HOMO level for efficient quantum dot light-emitting diodes," IEEE Electron Device Lett. **41**, 80–83 (2020).
24. H. H. Fong, A. Papadimitratos, and G. G. Malliaras, "Nondispersive hole transport in a polyfluorene copolymer with a mobility of 0.01 $cm^2\ V^{-1}\ s^{-1}$," Appl. Phys. Lett. **89**, 172116 (2006).
25. M. D. Ho, D. Kim, N. Kim, S. M. Cho, and H. Chae, "Polymer and small molecule mixture for organic hole transport layers in quantum dot light-emitting diodes," ACS Appl. Mater. Interfaces **5**, 12369–12374 (2013).
26. X. Qu, N. Zhang, R. Cai, B. Kang, S. Chen, B. Xu, K. Wang, and X. W. Sun, "Improving blue quantum dot light-emitting diodes by a lithium fluoride interfacial layer," Appl. Phys. Lett. **114**, 071101 (2019).
27. X. L. Dai, Z. X. Zhang, Y. Z. Jin, Y. Niu, H. J. Cao, X. Y. Liang, L. W. Chen, J. P. Wang, and X. G. Peng, "Solution-processed, high-performance light-emitting diodes based on quantum dots," Nature **515**, 96–99 (2014).
28. B. S. Mashford, M. Stevenson, Z. Popovic, C. Hamilton, Z. Q. Zhou, C. Breen, J. Steckel, V. Bulovic, M. Bawendi, S. Coe-Sullivan, and P. T. Kazlas, "High-efficiency quantum-dot light-emitting devices with enhanced charge injection," Nat. Photonics **7**, 407–412 (2013).
29. H. Zhang, N. Sui, X. C. Chi, Y. H. Wang, Q. H. Liu, H. Z. Zhang, and W. Y. Ji, "Ultrastable quantum-dot light-emitting diodes by suppression of leakage current and exciton quenching processes," ACS Appl. Mater. Interfaces **8**, 31385–31391 (2016).
30. W. D. Zhang, S. H. Ding, W. D. Zhuang, D. Wu, P. Liu, X. W. Qu, H. C. Liu, H. C. Yang, Z. H. Wu, K. Wang, and X. W. Sun, "InP/ZnS/ZnS core/shell blue quantum dots for efficient light-emitting diodes," Adv. Funct. Mater. **30**, 2005303 (2020).